Schweizerische Eidgenossenschaft
Confédération suisse
Confederazione Svizzera
Confederaziun svizra

Eidgenössisches Departement für
Umwelt, Verkehr, Energie und Kommunikation UVEK

Bundesamt für Energie BFE

Schlussbericht 30. September 2012

NUMERICAL SIMULATION, DESIGN, AND FABRICATION OF EXTREMELY THIN ABSORBER SOLAR CELLS

Auftraggeber:
Bundesamt für Energie BFE
Forschungsprogramm Photovoltaik
CH-3003 Bern
www.bfe.admin.ch

Auftragnehmer:
Zürcher Hochschule für Angewandte Wissenschaften
Technikumstrasse 9
CH-8401Winterthur
www.zhaw.ch

EMPA Thun
Feuerwerkerstrasse 39
CH-3602 Thun
www.empa.ch

Autoren:
Dr. Martin Loeser, Zürcher Hochschule für Angewandte Wissenschaften, loma@zhaw.ch
Dr. Laetitia Philippe, EMPA Thun, laetitia.philippe@empa.ch
Dr. Jamil Elias, EMPA Thun, jamil.elias@empa.ch

BFE-Bereichsleiter: Dr. Stefan Oberholzer
BFE-Programmleiter: Dr. Stefan Nowak
BFE-Vertrags- und Projektnummer: SI/500613-01

Table of Contents

1. Abstract

Our joint research focuses on combining both numerical and experimental methods to analyze, control and improve the optical characteristics of extremely thin absorber (ETA) solar cells. As a first step we produce and measure various reference devices with simplified geometries that are used as benchmark examples. On the computational side we extend our novel and cutting-edge three-dimensional full-wave optical simulation software OPUS 3-D in such way, that it allows for the numerical simulation of ETA solar cells and returns data that can directly be compared to experimental results. By showing that experimental and numerical data do not only agree for simple structures but also for very complex device designs we aim at establishing a combined framework helping to simplify the development of next-generation ETA solar cells. It is a unique approach that allows systematic analysis and design of the optical characteristics of ETA solar cells by combining elaborate experimental and numerical methods.

2. Introduction

The overall project goal is the development of a novel framework that – by combining experimental and numerical methods – facilitates the analysis and design of highly efficient ETA solar cells. To this end we aim at proving that our in-house three-dimensional full-wave optical simulation software can reproduce and predict experimentally determined optical characteristics – especially transmission and reflection spectra – of ETA solar cells for a very broad range of designs.

The first part of the project is dedicated to the production and experimental characterization of different reference devices on the one hand, and the extension of our in-house optical solver software OPUS 3-D on the other hand. This software tool utilizes a novel, finite-element based formalism, the Ultra-Weak Varia-tional Formulation, that has specifically been developed as a numerically efficient approach for analyzing light propagation in complex structures [1]. The second part of the project, aims at showing that – for a large variety of device designs and materials – there is good agreement between measured and simulated optical data, in particular, for both reflection and transmission spectra.

To illustrate the applicability of OPUS 3-D for the analysis of a broad range of scattering problems, we benchmark the simulation software with a large variety of standard problems such as planar multi-layer material interfaces or scattering from metallic or dielectric spheres. By showing the excellent agreement between the numerical solutions and the (semi-) analytical reference solutions we illustrate the simulator's validity.

In the next step of the benchmarking procedure, spectrally measured reflection and transmission coefficients, provided by EMPA, are compared to numerical data. This comparison is carried out for planar multi-layer devices with increasing complexity. In all cases excellent agreement between measured and simulated data could be achieved.

A last benchmarking step compares measured and simulated data for a very ad-vanced structure. Here, various ZnO nanowire arrays with different geometries, electro-deposited on a glass substrate, are investigated. Measured and simulated reflection and transmission spectra show, that both the length and the diameter of the nanowires have a very strong but distinct impact on the optical device characteristics. The good agreement between experiment and simulation underlines the simulator's ability to also investigate the characteristics of elaborate nano-structures.

3. Performed Work and Achievements

STATUS REPORT ON WORK PACKAGE 1: FABRICATION AND CHARACTERIZATION OF SAMPLE DEVICES.

Following the procedure outlined in the proposal, various simple reference structures were produced, and their optical characteristics were obtained experimentally. As the focus of this work package lies on benchmarking, we chose planar and nanostructured designs for which we measured both the transmission and reflection coefficients for a large range of optical frequencies.

Production of structures

Two classes of devices have been produced and measured within Work Package 1. The first reference design consists of a transparent glass substrate with a transparent conducting oxide (TCO) contact on top. For our purposes we have chosen a SnO2:F layer with a thickness of 1mm as TCO. The second class of devices additionally features an array of ZnO nanowires (NWs) on top of the TCO that serves as large band-gap n-type material for the electron transport. The TCO substrates (SnO2:F/glass) were purchased from Solaronix, Switzerland. The electrodeposition of ZnO NW was performed in a three-electrode electrochemical cell with the substrate (conducting glass) as the cathode, a Pt spiral wire as the counter electrode and a saturated calomel electrode (SCE) as the reference electrode. The electrolyte was an aqueous solution of ZnCl2 (5x10-4 M) and KCl (0.1 M), saturated with bubbling oxygen. The ultrapure water (18 MΩ.cm) was provided by a Millipore setup. The $ZnCl_2$ salt (Flucka, purity >98.0%) acts as a Zn2+ precursor. The substrates were conducting (10 Ω/square) glass/SnO2:F from Solaronix, Switzerland. For each working electrode, a geometric surface of 2 cm^2 was masked off prior to the electrodeposition experiments. As a first step, they were covered by a nanocrystalline ZnO buffer layer galvanostatically electrodeposited at room temperature (J = -0.15 mA/cm2, Q = 0.4 C/cm^2) using $ZnCl_2$ and KCl concentrations of 5x10-3 and 0.1 M, respectively. On top of the nanocrystalline ZnO buffer layer, the ZnO nanowire arrays were electrodeposited at 80 °C under –1 V constant potential. The charge density was 20 C/cm^2. In order to set the measured reflection and transmission spectra on a broader footing, the thickness of the ZnO layer has been varied between 670nm and 3360nm for the second class of devices. Thus, experimental data has been obtained for five different layer thicknesses.

Measurement of reflection and absorption spectra

After processing, the optical transmission (T) and reflectivity (R) spectra of the samples were measured at room temperature using an Ocean Optics HR2000+ES spectrophotometer connected to an integrating sphere. An Ocean Optics DH-2000-BAL served as light source. Two

different integrating spheres have been used – in one for the transmission and the other for the reflectivity measurements. When incident light passes through the sample (depending on its position) it can be diffracted in all directions inside the integrating spheres. A detector then collects the sum of all diffractions through an optical fiber, and this is how transmission or reflectivity spectra were obtained. After the measurements of T and R the absorption A can be obtained according to the Beer–Lambert law: A= 1–T–R. Further details can be found in our previous report.

STATUS REPORT ON WORK PACKAGE 2: EXTENSION OF SOFTWARE FEATURES IN THE EXISTING SIMULATOR OPUS 3-D.

During this project the 3-D full-wave finite-element solver OPUS 3-D has been extended substantially. As already indicated in the last report, the most important changes in the kernel are the inclusion of plane wave sources and the implementation of Perfectly Matched Layers (PML) to truncate the simulation domain. Whereas the first modification allows to model complex scattering and refraction problems, the latter change guarantees both computational efficiency and numerical accuracy. Thorough investigations reveal that reliable and accurate results can only be obtained if PML are employed at the boundaries of the simulation domain. These findings agree very well with what is reported in literature [1].

In addition, the post-processing unit of OPUS 3-D has also been extended and now allows easy computation of reflection, transmission, and absorption coefficients. With these additional features we are able to directly compare measured and simulated data. This is a major achievement because one of the project's main objectives is the development of a computationally efficient software tool whose results can easily be compared to measured data. Detailed comparisons and benchmarks will be discussed in the following sections.

It is among the main assets of the simulator that it is not only highly efficient for solving wave propagation problems in large domains, but that it also lends itself very well for the analysis of complicated multi-scale structures that cannot be examined with standard numerical tools (such as Finite-Difference Time-Domain FDTD or Finite Elements FEM). Thus, OPUS 3-D can be employed for the analysis of elaborate structures such as multi-layer devices featuring nanowire arrays working as light diffusors or light scattering centers. Yet, despite of the already highly efficient numerical algorithm that – to further reduce the computation times – has also been parallelized and runs simultaneously on more than 10 processors, it turned out that computation time is still a very critical issue when numerically analyzing advanced multi-scale structures. When computing the light propagation inside such devices the size of the numerical problem can easily exceed 4 million degrees of freedom, resulting in more than 25 GByte of required memory. If the computational task is then parallelized and simultaneously runs on many processors, an efficient speedup can only be achieved if the computational task is equally distributed among all these processors. Especially for the computation of reflection, transmission, and absorption spectra, where a large number of simulations needs to be run in order to cover the entire spectral range, computational efficiency is of utmost importance. To this end, a novel dynamic load-balancing scheme has been implemented that boosts the computational efficiency by another 30% and must therefore be considered as a major achievement of this project.

For a reference scattering problem, Figure 1 illustrates how load balancing boosts the computational efficiency when the numerical problem is distributed to many processors. The top plot shows the computation time as function of the number of processors. The red curve shows the behavior without load balancing, the blue curve shows the computation time when the novel load balancing scheme is employed. The dashed green curve represents the ideal case where the computation time would scale as 1/n. Up to 6 processors the combination of parallelization and load balancing yields a nearly ideal speedup – for larger problems this speedup is slightly less, which can be attributed to the increasing communication effort between the involved CPUs. The bottom plot compares parallelization with and without load balancing and displays the relative speedup that can be achieved by employing the novel load balancing scheme. For our benchmark this speedup lies between 25 and 30% if the numerical problem is distributed to more than three processors. Further investigations reveal that load balancing has an even stronger impact on the overall performance when the com-

plexity of the device increases. Thus, load balancing is an important step towards high numerical efficiency and especially pays off in cases where many optical simulations need to be run.

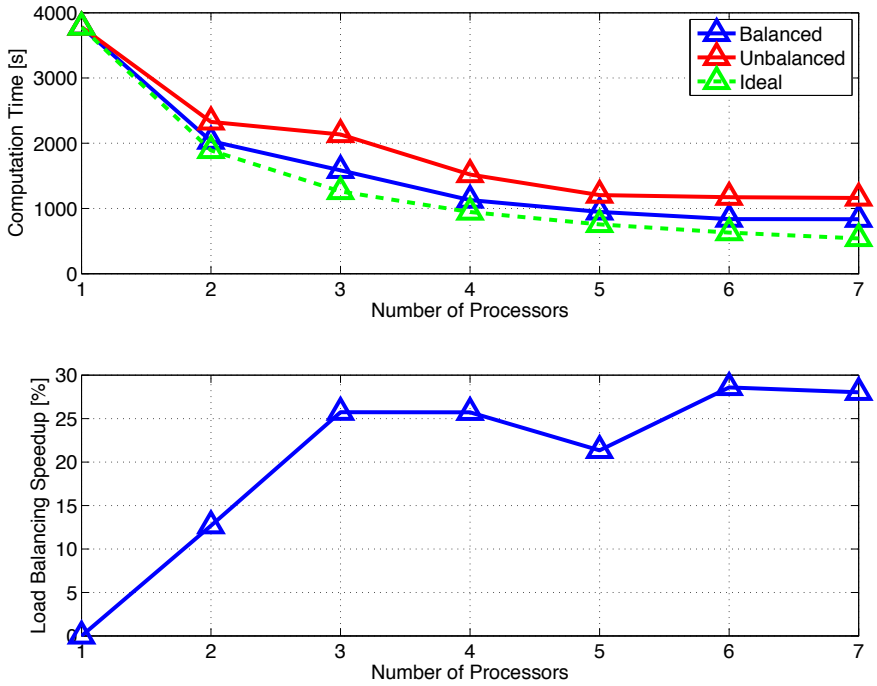

Figure 1: Parallel computing with and without load balancing. The top figure shows the computation time as a function of the number of processors for parallelization with load balancing (blue), without load balancing (red), and as a reference, the ideal 1/n behavior (green). The bottom curve shows the relative speedup (in %) that could be achieved when switching from unbalanced to balanced parallelization.

STATUS REPORT ON WORK PACKAGE 3: BENCHMARKING WITH (SIMPLE) REFERENCE STRUCTURES.

It is the aim of this section to show that OPUS 3-D is not only capable of computing the optical characteristics for a large variety of devices featuring complex geometries, but also, that these results feature high accuracy. Thus, we have chosen a clear and transparent benchmarking procedure that shows the capabilities of the simulator. In a first step, OPUS 3-D was benchmarked with a series of standard problems for which known solutions (either analytical or semi-analytical) exist. This step guarantees high transparency as everybody skilled with Matlab can reproduce and verify the results. In a second step, the simulation results were compared to measured data for various devices with increasing complexity.

Benchmark 1: Reflection and transmission spectra for layered structures

This benchmark is intended to illustrate that OPUS 3-D correctly computes reflection and transmission spectra for simple layered structures. We have chosen such simple structures as they allow for the easy computation of analytical reference solutions that can be obtained using a simple transfer-matrix method (TMM) approach. The benchmark is carried out for two different device designs. The first case is illustrated in Figure 2. Here, a plane wave impinges on a glass layer featuring a width of 525 nm. The glass layer is shown in transparent green whereas the Poynting vectors of the incident plane wave are shown as red arrows. Behind the glass layer there is an infinite layer of air.

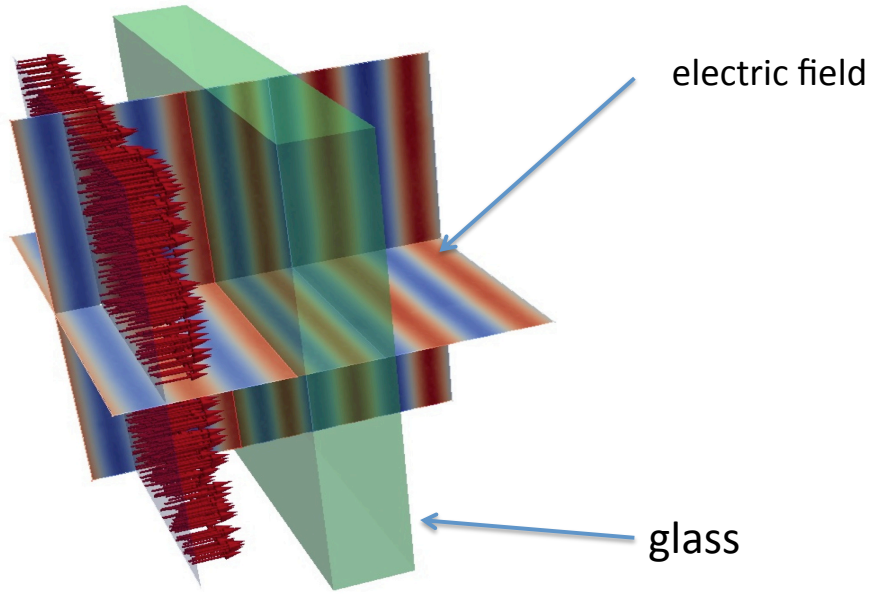

Figure 2: A plane wave impinging on a glass layer. The red arrows indicate the Poynting vector

Figure 3 shows a comparison of analytical and numerical results for both the transmission coefficient T and the reflection coefficient R. Here, the analytical reference solutions are indicated by solid lines whereas the numerical solutions, obtained from full-wave simulations with OPUS 3-D, are indicated as dashed lines. For the entire wavelength range from 400nm to 650nm there is excellent agreement between the numerical solution and the analytical reference solution.

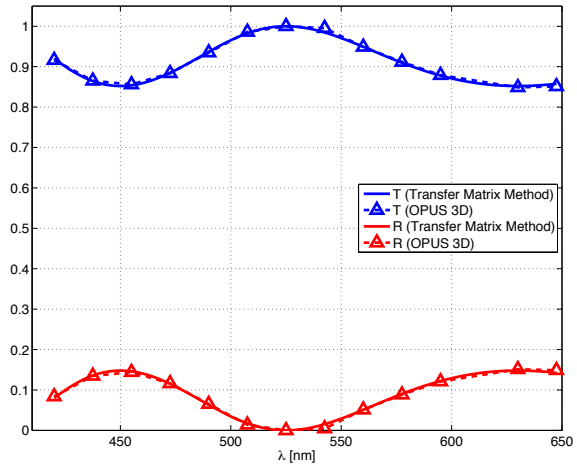

Figure 3: Comparison of transmission (blue) and absorption (red) spectra. The solid lines indicate the analytical reference solution, the dashed lines are the results from OPUS 3-D simulations.

In a next step, a more complicated device, that is designed as an anti-reflection filter operating at a wavelength of 570nm, is investigated. It is a planar multi-layer structure, consisting of two dielectric layers deposited on a glass substrate. Again, a plane wave impinges from free space on the structure, and both reflection and transmission coefficients are computed. Figure 4 shows the comparison between the analytical results obtained with TMM (solid lines) and the results from the 3-D full-wave simulations that were computed with OPUS 3-D (dashed lines). As before, for both R and T there is excellent agreement between the numerical and the analytical solution over a large wavelength range, from 400nm to 800nm. This illustrates the simulator's capability to correctly compute transmission, reflection, and absorption spectra for simple planar structures.

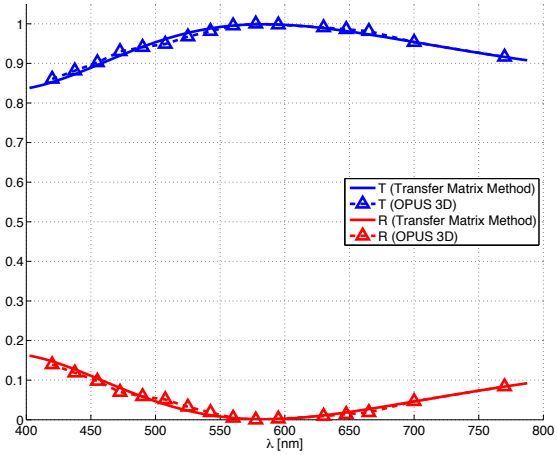

Figure 4: Comparison of analytical (solid) and numerical (dashed) solutions for a multi-layer anti-reflection filter. The red curves indicate the reflection coefficients, the blue curves are the transmission coefficients.

Benchmark 2: Scattering from a dielectric sphere

The following benchmark was set up in order to illustrate that OPUS 3-D is very well suited for the analysis of more challenging scattering problems with curved or bent geometries. As depicted in Figure 5 we analyze a plane wave that impinges on a dielectric sphere (with an index of refraction n=1.5) whose radius has a similar order of magnitude as the wavelength (r=2.5λ).

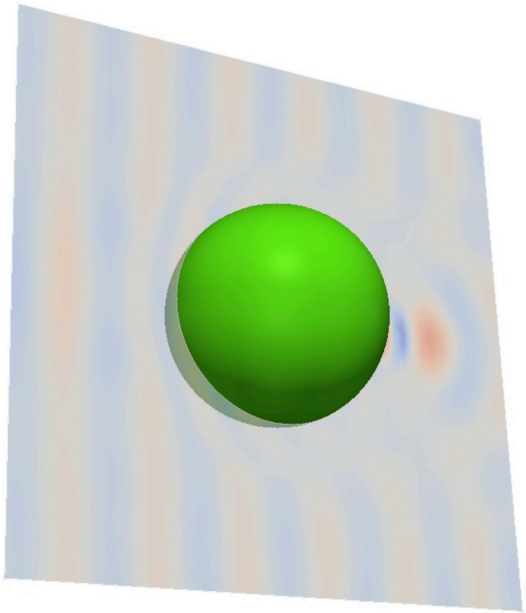

Figure 5: Mie scattering benchmark – a plane wave impinges on a dielectric sphere.

This benchmark is particularly challenging due to the sphere's curved surface. This example has not only been chosen to prove OPUS' ability to efficiently treat complex structures and material interfaces, but also because there exist well-known semi-analytical reference solutions – the Mie series. These reference solutions were computed in Matlab utilizing a freely available and thoroughly tested code. For the benchmarking procedure both the finite-element solution (OPUS 3-D) and the reference solution (Matlab) were evaluated and com-

pared on a three-dimensional computation domain. Whereas the CPU time for OPUS 3-D ranged around one hour the Matlab solution required a computation time of more than ten hours on the same computer. The comparison between both approaches is illustrated in Figure 6. To prove that there is not only a qualitative, but also a quantitative agreement, the same scales were utilized when plotting the electric fields both inside and outside the sphere. The error ranges around 3%.

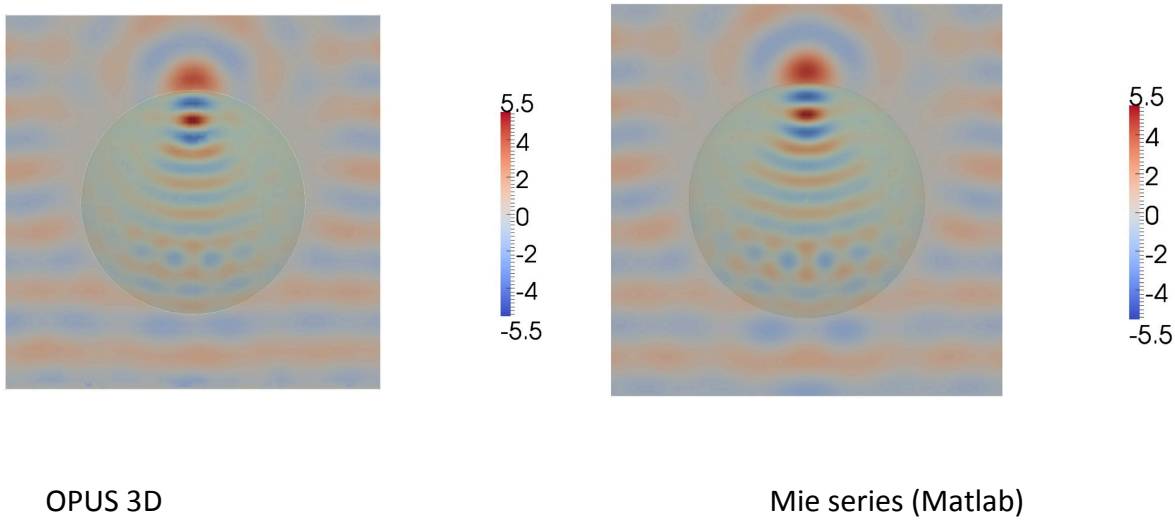

Figure 6: Comparison between numerical and semi-analytical solution

In order to show the general validity of the results a second benchmark was carried out. This time, however, the radius of the sphere was modified (r=1.5λ), and a metallic sphere replaced the dielectric sphere. The results of the second Mie scattering benchmark are depicted in Figure 7. Again, there is excellent agreement between the numerical solution, obtained with OPUS 3-D, and the semi-analytical reference solution computed in Matlab. This benchmark also illustrates that the simulator can account for complex metallic structures inside the simulation domain.

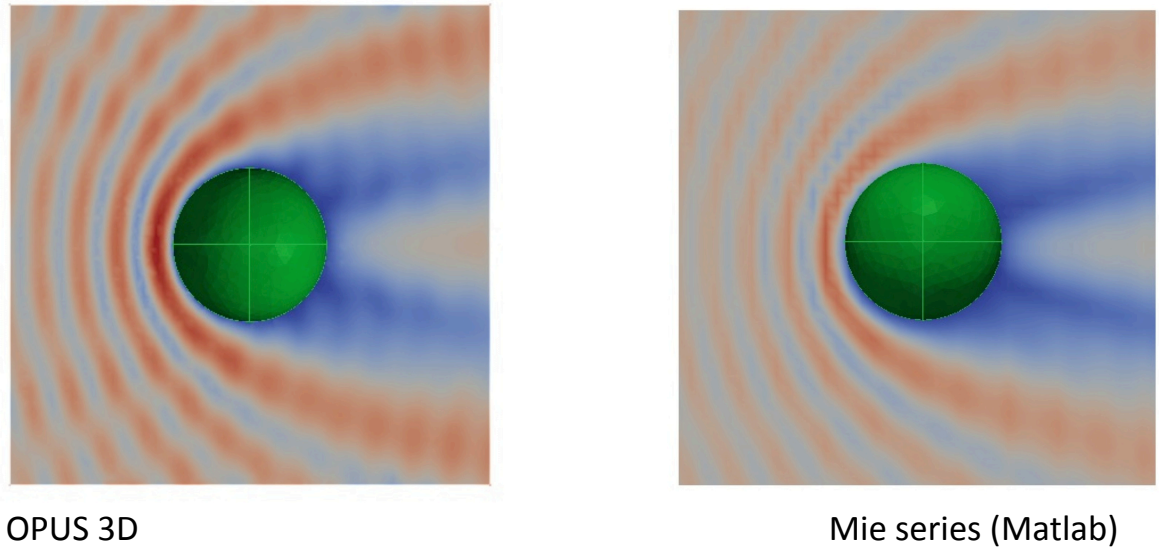

Figure 7: Scattering from a metal sphere. Comparison of numerical solution (left) and semi-analytical Mie series (right).

Extraction of refractive indices for multi-layer materials

As already outlined in the introduction, it is one of the project's main goals to illustrate the good agreement between measured and numerically computed optical characteristics for a large class of devices. Yet, prior to comparing measured and computed reflection and trans-

mission coefficients, it is of utmost importance to correctly describe the refractive indices of all involved materials as a function of the wavelength. Determining these values – either experimentally or numerically – is quite challenging a task for various reasons. First, there exist several uncertainties regarding the exact structure of the device, such as – owing to process variations – the thickness of the FTO layer on top of the glass substrate. Second, the measured devices can feature not only rough surfaces but also complex structures such as nanowires or urchin-shaped structures (as in [2]) that will yield in refractive indices that are different from those of bulk materials. Third, it is not always possible to experimentally analyze each material separately. For instance, the FTO can hardly be isolated and comes almost always deposited on a glass substrate. Thus, prior to comparing measured and numerically simulated reflection and transmission spectra it is mandatory to determine the refractive indices and layer thicknesses of all involved materials. In the following, we employ a two-step procedure to extract all relevant refractive index data from measured reflection and transmission coefficients (for a planar structure). First, we model the device as a material stack with infinite lateral dimensions and utilize a plane wave transfer-matrix-method to compute the reflection and transmission coefficients for each wavelength. The complex refractive indices of all involved materials, for example the FTO, the ZnO, and the glass, are modeled as standard Drude-Lorentz-oscillators that account not only for the refractive index but also for the material's absorption coefficient. For each of the materials the Drude-Lorentz model features several degrees of freedom, i.e., a parameter set to describe its optical characteristics. In a second step we employ a non-linear Leuvenberg-Marquardt optimization algorithm to determine the optimal model parameters by fitting the measured and numerically computed reflection and transmission coefficients. The entire procedure is implemented and evaluated using Matlab. Figure 8 shows the dispersion relation of the real part of the refractive index for three materials that typically occur in ETA solar cells. These data were obtained after a successful optimization procedure. They are further employed when simulating devices featuring more complex designs, e.g., arrays of nanowires.

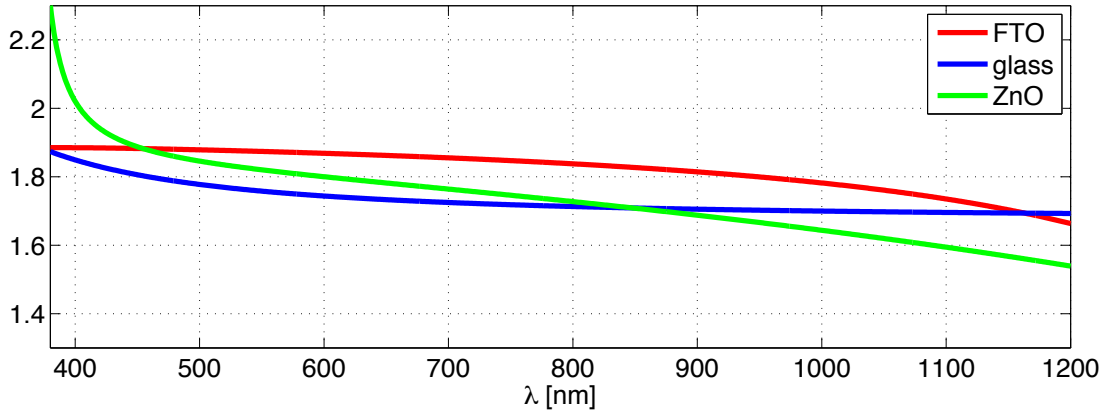

Figure 8: Refractive indices of FTO, glass, and ZnO as functions of the wavelength.

Benchmark 3 – Comparison with measured data, glass-FTO-structure

After determining the refractive indices, the first comparison between measured and simulated data is carried out for a simple planar reference device. It features a glass substrate covered by a layer of transparent conducting oxide FTO. The FTO layer thickness ranges around 700nm. For a broad wavelength range, from 300nm up 1200nm, the optical characteristics of this structure are analyzed both experimentally and numerically. During the experiment a monochromatic plane wave impinges on the structure and both reflected and ab-

sorbed power are measured simultaneously. The measured data are indicated in Figure 9 (solid lines), where the red curve corresponds to the reflection coefficient whereas the blue curve shows the transmission coefficient. For a direct comparison to simulated data, the same structure is modeled in OPUS 3-D, and both R and T are computed in a post-processing step after the 3-D full-wave simulation finishes. The most important input parameters for the numerical simulation are the device geometry and the materials' refractive indices. The latter were obtained from the data displayed in Figure 8.

The comparison between simulated and measured data is shown in Figure 9. The solid lines indicate measured data, the dashed curves show both the computed reflection and transmission spectra, and the triangles indicate for which wavelengths these values have been computed. The plot clearly shows the excellent agreement between simulated and measured data for the entire wavelength range.

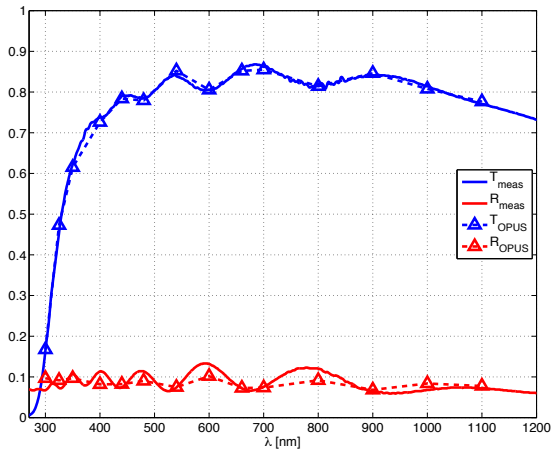

Figure 9: Comparison between measured (solid) and simulated (dashed) reflection and transmission spectra for a planar glass-FTO structure. The measured data are provided by EMPA Thun.

Benchmark 4 – Comparison with measured data, glass-ZnO-FTO-structure

Here, a more elaborated device is being analyzed. It is similar to the previous reference device, but this time the structure features an additional compact layer of ZnO with a thickness of 840nm. The benchmarking procedure is identical to Benchmark 3 – for a broad wavelength range we measure and simulate the reflection and absorption spectra. A direct comparison of these data is shown in Figure 10. The solid lines indicate measured reflection and transmission coefficients whereas the dashed lines indicate simulation results. As in the previous case there is excellent agreement between simulated and measured data over the entire wavelength range.

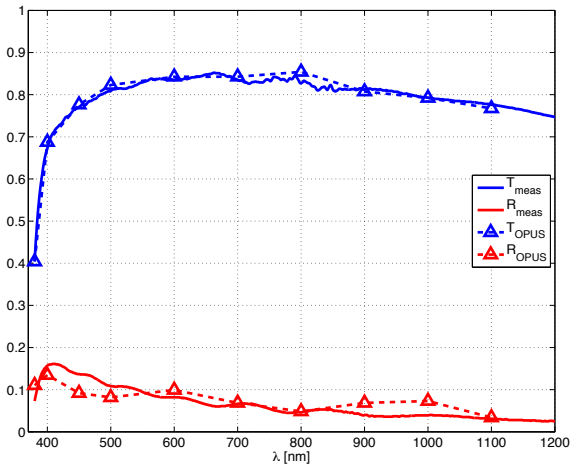

Figure 10: Comparison between measured (solid) and simulated (dashed) reflection and transmission spectra for a planar glass-ZnO-FTO structure. The red curves indicate measured and simulated reflection coefficients, the blue curves show the transmission coefficients. EMPA Thun provided the measured data.

STATUS REPORT ON WORK PACKAGE 4: SIMULATION OF MORE REALISTIC STRUCTURES AND COMPARISON TO MEASURED DATA

The previous benchmarks illustrated that OPUS 3-D is capable of computing both reflection and transmission spectra in such way that they can easily be compared to measured data. After having shown the simulator's accuracy by comparing the numerical results to either analytical reference solutions or measured data, the following section illustrates how the simulator can help to investigate and under-stand experimental findings that cannot be explained or reproduced with simple one-dimensional or analytical models.

The structure we investigate in the following is a ZnO nanowire array whose detailed description can be found in [3]. An SEM image of the structure is shown in Figure 11. Here, various arrays of ZnO nanowires were electro-deposited on glass substrates featuring a conducting SnO2:F layer.

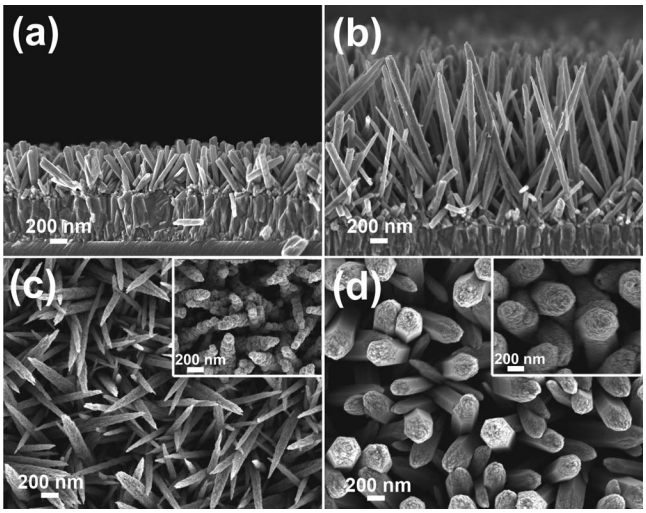

Figure 11: ZnO nanowires electro-deposited on a glass conductive substrate (FTO).

In order to control each nanowire dimension separately (diameter and length) we have used our reported methods for electrodeposition of ZnO nanowire arrays with tailored dimensions (see also [4]). In the following, the electrodeposition conditions as well as the dimensions' variation are briefly presented in table 1 and 2 (for length and diameter variation, respectively). For the series where we fix the diameter and vary the length the fixed conditions are: [KCl] = 1 M, saturated O2, T = 80 °C, V= -1 V vs ECS. For the series where we fix the length and vary the diameter the fixed conditions are: saturated O2, T = 80 °C, V= -1 V vs ECS.

Table 1: Varied nanowires' length at different electrodeposition conditions.

Length (µm)	Diameter (nm)	[ZnCl2] (M)	Q (C/cm2)*
0.5	95	5x10-4	5
0.9	103	5x10-4	10
1.5	90	1x10-4	20
2.0	95	1x10-4	38

Table 2: Varied nanowires' diameter at different electrodeposition conditions.

Diameter (nm)	Length (µm)	[ZnCl2] (M)	[KCl] (M)	Q (C/cm2)*
105	1.52	1x10-4	1	38
133	1.40	5x10-4	3,4	2.5
180	1.44	5x10-4	1	10
330	1.50	5x10-4	3,4	4

These nanowires differed with respect to thickness (diameter from 105 to 330 nm) and length (from 0.5 to 2 µm). Technical details about the elaborate measurement procedure can be found in our last report.

The experiments revealed that both the length of the nanowires and their diameter have a very strong but distinct impact on the reflection and transmission spectra. The measurements show that – leaving the nanowire diameter constant – an increase in nanowire length generally results in significantly higher reflection while leaving the peak reflection wavelength unchanged. In contrast, increasing the width of the nanowires while keeping their length constant not only broadens the reflection spectrum but also leads to a significant red shift of the absorption peak wavelength. Both experimental findings are outlined in Figure 12.

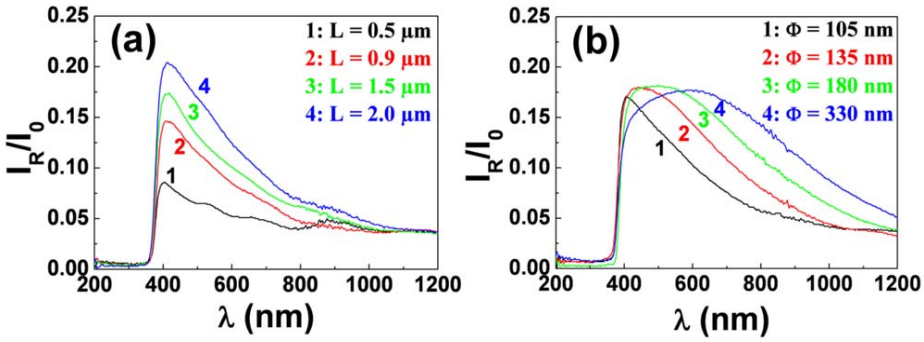

Figure 12: Impact of nanowire length and diameter on the reflection coefficient; measured by EMPA Thun. Subplot a) shows the reflection spectra for a constant wire diameter of 100nm – the length is gradually increased from 500nm to 2000nm. Subplot b) shows the reflection coefficients when the nanowire length is kept constant at 1500nm and the diameter is increased from 105nm to 330nm

It is the goal of this benchmark to show that a numerical analysis of such nano-wire structures confirms the essential experimental findings. Clearly, this is a problem that cannot be analyzed with simple one-dimensional approaches or ray-optical approximations but mandates the use of 3-D full-wave simulations as the devices feature complex three-dimensional sub-wavelength nanowires. A particular challenge arises during the numerical analysis, as this is a multi-scale problem. On the one hand we have to treat a rather large simulation domain with a size of several wavelengths in any of the three spatial dimensions. On the other hand, the nanowires featuring a diameter ranging around 100nm are sub-wavelength structures that need to be accounted for. It is the combination of large simulation domains and small sub-wavelength structures that makes the numerical investigation of these structures a most challenging task. Such multi-scale problems cannot be efficiently treated with standard numerical tools such as Finite Elements or Finite-Difference Time-Domain. In both cases the computational cost would be much too high for an efficient numerical treatment.

The computational model used for the numerical analysis with OPUS 3-D is depicted in Figure 13. Similar to what was done on the experimental side we modified both length and diameter of the nanowires and computed the reflection and transmission coefficient for a large wavelength interval ranging from 400nm to 1000nm. The efficient numerical model guaranteed moderate computational requirements even for very detailed and accurate models. All numerical problems featured between 2'500'000 and 4'500'000 degrees of freedom, which translated to a memory consumption of some 25 GByte. Employing the newly developed

load balancing scheme the computation time ranged around 80 minutes when distributed to 12 CPUs.

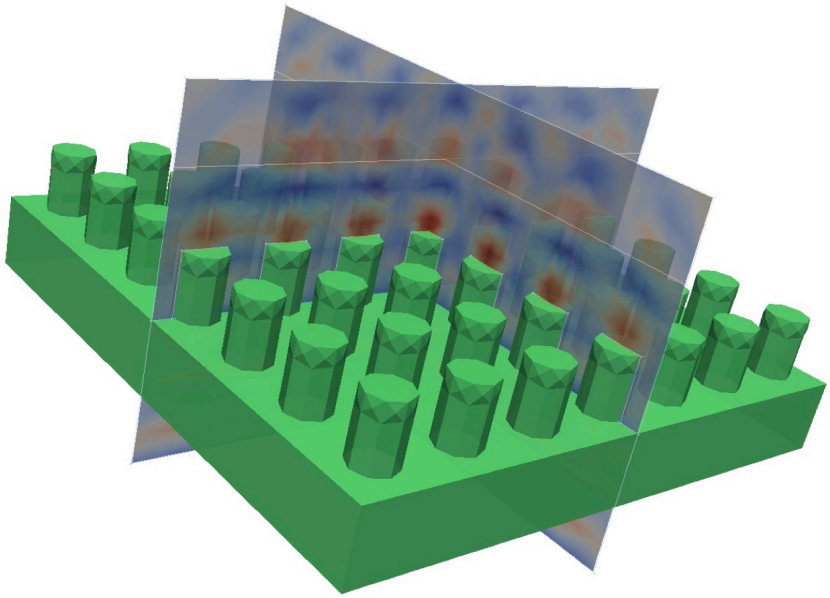

Figure 13: Computational model for analyzing the impact of the nanowire structure on the optical device characteristics.

The key findings of the simulations are illustrated in Figures 14 and 15. Figure 14 shows how the reflection spectrum evolves when the diameter of the nanowires is kept constant at 200 nm whereas the length increases from 500 nm to 1500 nm. Similar to what is observed during the measurements we see that the reflection coefficient strongly increases for wavelengths between 400 nm and 600 nm whilst the spectral position of the reflection peak remains approximately constant at about 500 nm. This is in excellent agreement with measured data.

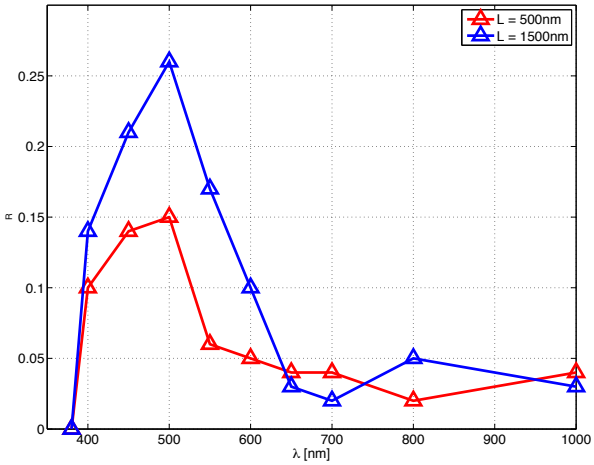

Figure 14: Simulation result - impact of nanowire length on the reflection coefficient. The diameter of the nanowires is kept constant at 200nm. An increase in nanowire length leads to a strong increase of the reflection coefficient. The peak wavelength remains constant at 500nm.

If – on the other hand – the length of the nanowires is kept constant at 1500 nm whereas their diameter is increased from 200 nm to 290 nm the simulation reveals two significant changes in the reflection spectrum. These changes are depicted in Figure 15. First, the in-

creasing width leads to a broader reflection spectrum. Second, the new absorption spectrum shows a clear red shift – its peak wavelength shifts from 500 nm to 600 nm. Again, this is in very good agreement with measured data.

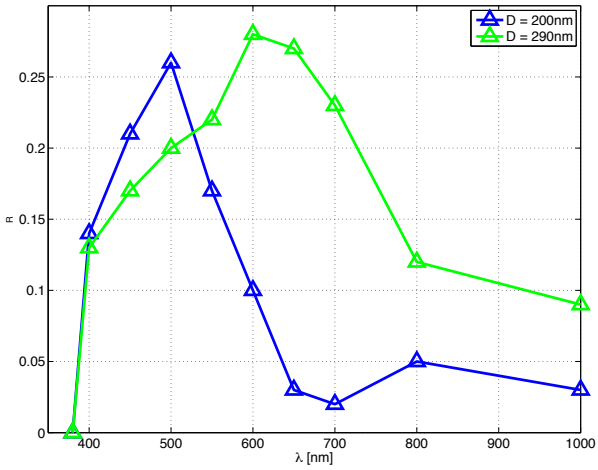

Figure 15: Simulation result - impact of nanowire diameter on the reflection coefficient. The nanowire length is kept constant at 1500 nm. The diameter is increased from 200 nm to 290 nm.

Summing up, a comparison to the measured results clearly shows that both key findings – the increase of reflection with increasing length and both the red shift and the broadening of the spectrum with increasing width – can be reproduced and analyzed using numerical simulations. Here, we have good agreement not only qualitatively, but also quantitatively.

NATIONAL AND INTERNATIONAL COOPERATION

As already outlined in the last report, the success of the entire project is strongly related to the efficient and fruitful national collaboration between EMPA Thun and the Zurich University of Applied Sciences. The communication and cooperation strategy has not changed since the last report. Thus, all work packages that could be carried out independently were split between the partners. Other tasks that required far-reaching strategic discussions were decided upon by all partners in order to achieve the best possible results.

In addition, this research project has also arisen strong international interest. The project team was approached by an international innovation magazine and invited to publish an article about their work that is to appear in a special edition focusing on cutting edge Swiss research. This article will be available for more than 30’000 readers in Europe and the INCO countries and is to appear during the next couple of months.

4. Summary and Outlook

We have successfully demonstrated that our novel simulation software OPUS 3-D is well suited for the numerical analysis of elaborate ETA solar cell structures. By showing the good agreement between measured and simulated optical data for a broad variety of designs we could illustrate that our approach – combining measured and simulated data – is well suited for the analysis and design of next-generation ETA solar cells. Among the next possible steps are the analysis and design of even more complex structures such as solar cells featuring urchin-like nanostructures or the transition to combined electro-optical simulations.

5. References

[1] T. Huttunen, M. Malinen, P. Monk: Solving Maxwell’s Equations using the Ultra-Weak Variational Formulation, Journal of Computational Physics, Edition 223, pages 731 – 758, 2007.

[2] Elias, J. , Lévy-Clément, C. , Bechelany, M. , Michler, J. , Wang, G.-Y. , Wang, Z. , Philippe, L. Hollow urchin-like ZnO thin films by electrochemical deposition, Advanced Materials , Volume 22, Issue 14, 12 April 2010, Pages 1607-1612

[3] R. Tena-Zarea, J. Elias, C. Levy-Clement: ZnO nanowire arrays: Optical scattering and sensitization to solar light, Applied Physics Letters, 93, 2008

[4] Elias, J., Tena-Zaera, R., Lévy-Clément, C., Electrochemical deposition of ZnO nanowire arrays with tailored dimensions, Journal of Electroanalytical Chemistry, Volume 621, Issue 2, September 15, 2008, Pages 171-177